Electron-Spin Resonance Study of Aggregation of Gramicidin in Dipalmitoylphosphatidylcholine Bilayers and Hydrophobic Mismatch

Mingtao Ge and Jack H. Freed
Department of Chemistry and Chemical Biology, Baker Laboratory, Cornell University, Ithaca, New York 14853 USA

ABSTRACT The effect of aggregation of gramicidin *A′* (GA) on the phase structure of dipalmitoylphosphatidylcholine (DPPC) multilamellar vesicles was studied by cw-ESR using a chain-labeled lipid (16PC) at temperatures between 30° and 45°C that span the main phase transition of DPPC. Boundary lipids were observed only in dispersions with GA/DPPC molar ratios >1:15, where GA aggregates. Detailed fits by nonlinear least squares (NLLS) methods are consistent with the boundary lipid being characterized by a large negative order parameter (~ -0.4), indicative of a dynamic bending of the end of the acyl chain, and a substantially reduced motion, about an order of magnitude slower than that of the bulk lipid. The NLLS analysis compares favorably with a recent two-dimensional Fourier transform ESR study on DPPC/GA vesicles, which accurately discerned the bulk lipid. The detailed ESR observables are discussed in terms of the ordering effect of GA at low concentration of GA, the dissociation of the GA channel and the dynamic bending of the end chain segment of boundary lipid at high concentration of GA, and of H_{II} phase formation induced by GA. It is suggested that these phenomena can be interpreted in terms of the combined effects of partial dehydration of the lipid headgroup by the GA and of the hydrophobic mismatch between GA and DPPC molecules. Substantial hysteresis is observed for heating versus cooling cycles, but only for a GA/DPPC molar ratio >1:15. This is consistent with the aggregation of GA molecules at high concentrations.

INTRODUCTION

Lateral aggregation is crucial for some intrinsic membrane proteins in order to perform their biological functions. For example, clustering of receptors of the epidermal growth factor is required for the initiation of DNA synthesis (Schreiber et al., 1983). Cross-linking or aggregation of insulin receptor is important for insulin action (Kahn et al., 1978). Also, cross-linking of the IgE receptor complex in mast cells is necessary for signal transduction (Robertson et al., 1986; Holowka and Baird, 1996). However, the molecular details of how such aggregation triggers the intracellular processes remains largely unknown.

Aggregation of proteins may modulate the phase structure of biomembranes (de Kruijff et al., 1985). It is vital for a living cell to keep its plasma membrane integral; however, for some biological processes such as endocytosis, exocytosis, and envelope virus infection, nonbilayer structures may be needed locally or transiently. These structures could be induced by aggregation of some specialized proteins. For example, microaggregation of Sendai viral glycoproteins and their accumulation in regions of contact between cells may play an essential role in envelope-cell fusion and in the induction of the cell-cell fusion (Henis, 1993). Therefore, studies of how the aggregation of membrane protein modulates the membrane phase structure would help to understand the molecular mechanism of those membrane protein-associated biological events. For this purpose, gramicidin *A′* (GA) is a good model system, because its H_{II} phase inducing activity is directly related to the aggregation of GA molecules (Killian and de Kruijff, 1985a, 1988; for a recent review, see Killian, 1992), and the H_{II} phase formation is of fundamental relevance for many biological processes taking place in biomembranes. This motivates our interest in the aggregation of GA. It is our objective that by studying the aggregation of GA as well as GA-induced H_{II} phase formation, insights will be provided into the relationship between aggregation of membrane proteins and nonbilayer phase formation that may initiate important biological processes.

It is known that GA induces an H_{II} phase in phosphatidylcholine (PC) model membranes (Van Echteld et al., 1982). It lowers the onset temperature of the bilayer to H_{II} phase transition for phosphatidylethanolamine (PE) (Van Echteld et al., 1981; Killian and de Kruijff, 1985a). It induces fusion of large unilamellar vesicles of DOPC when the molar ratio of GA/DOPC exceeds 0.01, and a small amount of H_{II} phase of DOPC could be detected at a molar ratio of 0.02 (Tournois et al., 1990). It is also known that GA can dissolve in DOPC dispersions up to a molar ratio of 1:15 of peptide to lipid. Upon exceeding this ratio, aggregation of GA occurs, resulting in a macroscopic phase separation. A lamellar phase with a DOPC/GA ratio of 15 and an H_{II} phase highly enriched in GA co-exists (Killian et al., 1987). Dipalmitoylphosphatidylcholine (DPPC)/GA systems have also shown H_{II} phase formation (Watnick et

Received for publication 8 September 1997 and in final form 30 September 1998.

Address reprint requests to Dr. Jack H. Freed, Department of Chemistry and Chemical Biology, B52 Baker Laboratory, Cornell University, Ithaca, NY 14853. Tel.: 607-255-3647; Fax: 607-255-0595; E-mail: jhf@msc.cornell.edu.

Abbreviations used: IgE, immunoglobulin E; AFM, atomic force microscopy; Chol, cholesterol; DMPC, 1,2-dimyristoylphosphatidylcholine; DOPC, 1,2-dioleoylphosphatidylcholine; DOXYL, 4′,4-dimethyloxazolidine-N-oxyl; HB, homogeneous broadening; IB, inhomogeneous broadening; MOMD, microscopic order and macroscopic disorder; NLLS, nonlinear least squares; PEG, polyethylene glycerol; POPC, 1-palmitoyl-2-oleoylphosphatidylcholine; POPE, 1-palmitoyl-2-oleoylphosphatidylethanolamine.

0006-3495/99/01/264/17 $2.00

al., 1990). Line type and cross-linked line type clusters of GA molecules were directly observed in supported bilayers of PC lipid (including DPPC) containing various amount of GA by atomic force microscopy (Mou et al., 1996). It was shown that GA-induced H_{II} phase formation is acyl chain length-dependent, so the hydrophobic mismatch between the thickness of the acyl chain of lipid bilayers and the length of the GA channel is important for the H_{II} phase formation (Van Echteld et al., 1982). A comprehensive five-step model for GA-induced H_{II} phase formation was suggested (Killian and de Kruijff, 1988), which involves dissociation of GA channels in the lamellar phase, followed by lateral self-association of GA monomers into curved aggregates. Concomitantly lipid molecules reorganize around the curved aggregates, thus forming an H_{II} phase. In the model, the dissociation of a GA channel was assumed to be a prerequisite for GA aggregation. However, no details were given of how the GA channel is destabilized as more GA molecules are incorporated into the bilayers. Although it was observed consistently by various techniques that low [GA] increases the ordering of lipid bilayers and high [GA] reduces the ordering of lipid bilayers (Rice and Oldfield, 1979; Lee et al., 1984; Cortijo et al., 1982; Short et al., 1987; Cornell et al., 1988), the mechanism of the ordering effect of GA at low [GA] is still not clear.

In a previous ESR study of DPPC/GA interactions (Ge and Freed, 1993), we found that a second, broad component develops in the spectra from spin labels 16PC and 10PC in DPPC/GA dispersions, when the molar ratio of GA to DPPC is $>$1:15. This is more clearly seen for the spectra from 16PC than from 10PC, but is not seen for the spectra from 5PC (Ge and Freed, 1993). As will be shown below, these spectra revealed interesting acyl chain conformation changes induced by GA. However, due to the ambiguity of the simulations performed for these cw-ESR spectra, the interpretation proved to be inconsistent with those from the recent 2D-ELDOR study of DPPC/GA dispersions with lipid-to-peptide molar ratio of 5 (Patyal et al., 1997).

While potentially very informative (Meirovitch et al., 1984; Ge and Freed, 1993; 1998), the proper simulation of cw-ESR spectra from membrane vesicles poses a particular challenge, because of their limited resolution. This arises because the spectra are characteristic of the lipids in the membrane being microscopically well-aligned or ordered within the vesicles, but the macroscopic sample, composed of vesicle dispersions, provides a random distribution of directions of alignment, (i.e., directors, which are perpendicular to the bilayer plane). We refer to this as MOMD. The superposition of spectra from all orientations leads to a major source of inhomogeneous broadening that relates to the degree of microscopic ordering. However, it tends to mask the homogeneous broadening relating to the molecular dynamics. The fitting of the resultant spectra tends to be ambiguous. One solution to this problem is to use macroscopically aligned samples, which may be studied over a variety of tilt angles. In fact, this was done in the studies of Ge et al. (1994), but only small mole percents of macromolecule in general, and GA in particular (e.g., $\sim$2–4 mol %), could be successfully incorporated. In that work (Ge et al., 1994) we also pointed out the significant differences between the effects of GA on oriented samples versus membrane vesicles. Thus, one must deal with the ambiguities of the cw-spectra from vesicles in order to learn about the effects of GA aggregation in such morphologies.

In our recent analysis of the nonlinear least squares fitting of spectra from aligned samples versus vesicles (Budil et al., 1996), it was found in test studies that the uncertainties from the MOMD fits are 5–10 times larger than those from the fits to the aligned samples as a result of the macroscopic disorder. The ambiguity that can exist in fitting MOMD spectra was illustrated in another test, where sample spectra were fit to an incorrect or more approximate model. The MOMD spectra were found to be more forgiving of the inaccuracies in the model, consistent with a given MOMD spectrum being able to tolerate a range of different models. This ambiguity in being able to be fit by different models had previously been illustrated by us (Ge and Freed, 1993) in model simulations which, however, did not have the benefit of the latest least-squares algorithms, so they had to rely heavily on trial-and-error procedures.

The ambiguity and limited resolution of MOMD spectra from membrane vesicles has been overcome in the form of two-dimensional Fourier-transform (2D-FT) ESR (Crepeau et al., 1994; Lee et al., 1994), and a study of a vesicle system containing GA has recently been completed (Patyal et al., 1997). That study provided reliable ordering and dynamic parameters for the bulk lipids in the liquid crystalline phase. It was less successful in the gel phase, presumably because of the much greater resolution 2D-FT-ESR provides to the motional model, e.g., the role of the internal chain dynamics, which is slower, hence less completely averaged, in the gel phase. (That is, the 2D-FT-ESR spectrum is much less tolerant of an imperfect model.) Also, in that initial study, no significant evidence of the boundary lipid, which is clearly manifest in the cw-ESR spectra, was present. This is undoubtedly due to the much shorter T_2 values of the slower tumbling boundary lipid, which results in the more rapid decay of its ESR signal during the spectrometer dead time, as pointed out by Patyal et al. (1997).

The aim of this study was to examine how the aggregation of GA induces changes in lipid phase structure. Specifically, we are most concerned with the effect of aggregation of GA on the boundary lipid as monitored by the changes in the amount and nature of boundary lipid. For the present, this could be accomplished most readily by cw-ESR studies accompanied by least-squares fitting. The ambiguity in fitting could be reduced by utilizing parameters that are reasonably consistent with the results for the bulk lipid obtained from the 2D-FT-ESR study for a 5:1 lipid/GA mole ratio. Additionally, we adopt the point of view that the simulations are most useful in interpreting trends rather than in their absolute significance. [It is interesting to note that the results we obtain suggest there could be subtle effects on the 2D spectra from the boundary lipid, even though they do

not make substantial contributions. The present study also shows how the presence of boundary lipid can be enhanced. When this is coupled with very recent advances in 2D-FT-ESR sensitivity and dead times (Borbat et al., 1997), it will be possible in the future to benefit from combined cw-ESR and 2D-FT-ESR studies to more rigorously characterize the boundary lipid, and how it is affected by aggregation of GA.]

In this paper we will examine the following matters. 1) The variations in ordering of bulk lipid with [GA], the variations in ordering of boundary lipid with temperature, and hysteresis effects at high [GA], which show that GA molecules aggregate for ratios of GA/DPPC >1:15, consistent with previous studies (Chapman et al., 1977; Killian and de Kruijff, 1985a). 2) With the aggregation of GA, our results indicate that there is a dynamic bending at the end of acyl chain of the boundary lipid, which we believe is responsible for the disordering effect at high [GA]. The dynamic bending is revealed by a large negative order parameter of 16PC in the boundary lipid. 3) The ordering effect at low [GA], the dissociation of GA channels, and the dynamic bending of acyl chains at high [GA] are interpreted in terms of both the dehydration effect of GA and the hydrophobic mismatch between GA and DPPC molecules. This is clarified by a comparison between the ordering effect on the acyl chains by GA and by water-soluble polymers, such as PEG. 4) We present evidence that boundary lipid molecules are associated with GA aggregates, whereas the bulk lipid molecules are associated with GA channels. The biological significance of the boundary lipid as observed in previous ESR studies on the lipid/protein interactions is discussed. 5) We further suggest, in a comparison with other studies (e.g., Killian et al., 1987; Watnick et al., 1990), that the boundary lipids we observe for GA/DPPC > 10 are in the H_{II} phase, and we discuss implications of our results in this light.

MATERIALS AND METHODS

Materials

DPPC and spin-labeled lipid 16PC were obtained from Avanti Polar Lipids, Inc. (Birmingham, AL) and GA was purchased from Sigma (St. Louis, MO). All materials were used without further purification.

Sample preparation and ESR spectroscopy

Since the spin-labeled 16PC is the one most sensitive to the aggregation of GA (its spectra most clearly show the broad component at high [GA]; Ge and Freed, 1993), it was used in our present study. For purposes of comparison with our previous cw-ESR studies (Tanaka and Freed, 1985; Ge and Freed, 1993; Ge et al., 1994) and with our recent 2D-FT-ESR study (Patyal et al., 1997), in which DPPC was consistently used, this lipid was used for the present study. As will be seen later, a comparison with the 2D-FT-ESR study is important in overcoming the ambiguity in the cw-ESR study. The choice of the temperature range for this study from 30°C to 45°C, which is around the gel-to-liquid crystalline phase transition temperature of DPPC, is based on the following considerations. It was suggested (Chapman et al., 1977, 1979) that at high [GA], as the temperature is lowered and the lipids crystallize, GA molecules will be excluded from the crystallizing lipid, causing GA aggregates to form. Ge et al. (1994) suggested that GA disaggregates at temperatures slightly below the gel-to-liquid crystalline phase transition in macroscopically oriented DPPC bilayers containing 2 mol % GA. Therefore, changes in ESR spectra at temperatures around the gel-to-liquid crystalline phase transition of lipid would be more sensitive to any possible changes in lipid phase structures. We paid special attention to changes in ESR spectra at and near the phase transition temperature. As will be shown later, we did observe a sharp change in the order parameter of the boundary lipid at the transition temperature.

For comparison with the relevant previous studies, the procedure for preparing GA/DPPC dispersions was essentially the same as the one we used previously (Ge and Freed, 1993; Patyal et al., 1997) and that used by Watnick et al. (1990) and by Killian and de Kruijff (1985a, b) and Killian et al. (1987). That is, measured amounts of DPPC and GA were dissolved in chloroform/methanol (2:1 v/v; Killian and de Kruijff, 1985b). The concentration of 16PC added was 0.5 mol % of the DPPC. The solvent was evaporated by nitrogen gas flow. To ensure complete removal of the solvent the sample was pumped overnight, then excess water was added. The sample was hydrated at room temperature for two days. Bouchard et al. (1995) showed that for a 1:1 chloroform/methanol solution, the GA incorporated into the lipid membrane is initially a mixture of two conformers: a non-channel-forming (non-CF) double-stranded (DS) antiparallel helical dimer and a CF single-stranded (SS) N-N terminal helical dimer. Use of 2:1 chloroform/methanol solution would be expected to favor the latter over the former due to the increased polarity of the solvent. The thermodynamically stable form in the lipid membrane is the CF conformer, and in time the DS conformer converts to the CF one, a process accelerated by incubation at a temperature of ~60°C (yielding full conversion in DMPC ~7 h after the sample had initially been dissolved in ethanol; Bouchard et al., 1995). We allowed incubation for at least several days at room temperature, which appears similar to the procedure of Killian and de Kruijff (1985b). This procedure was necessary for us to perform heating versus cooling cycle experiments. We have found that the reproducibility of the ESR spectra from our samples is very good, even after variable periods of incubation, including storage at 4°C, for several months. Based on this and the previous studies of Killian and de Kruijff and of Watnick et al. we are reasonably confident that the GA is primarily in the CF conformer in our ESR studies.

The ESR spectra were taken on a Bruker ER-200 spectrometer at a frequency of 9.55 GHz and the magnetic field was calibrated with a ER300 gaussmeter. The temperature was measured with a Varian temperature controller with an accuracy of ±0.5°C by means of a copper-constantan thermocouple inserted at the bottom of the cavity.

Definitions of parameters used in the simulation

The parameters used in the simulations (Schneider and Freed, 1989) are briefly summarized here. First, we define axis frames used in the simulations: the molecular frame (x', y', z'), the local director frame (x'', y'', z''), the magnetic frame (x''', y''', z'''), and the laboratory frame (x, y, z), which are shown schematically in Fig. 1. In Fig. 1 *A* a fairly well-ordered hydrocarbon chain (part of an acyl chain of a lipid molecule) is shown with a preferential orientation along the local director (z'' axis) and a DOXYL nitroxide radical is attached near the end of the chain. Fig. 1 *B* shows a hydrocarbon chain which has the same structure as in Fig. 1 *A*; its overall preferential orientation remains unchanged, but the end chain segment is bent. The molecular frame (x', y', z') is the frame in which rotational diffusion constants $R_\perp$ and $R_\parallel$ are defined, which characterize the dynamics of the acyl chain. $R_\perp$ and $R_\parallel$ are the principal values of an axially symmetric rotational diffusion tensor for the nitroxide moiety attached to the chain segment. Specifically, they represent the rotational diffusion rates around an axis perpendicular and parallel to the axis of the chain segment, respectively, i.e., around the z' and x' (or y') axes, respectively. In Fig. 1, *A* and *B* only the z' is shown. The principal axis frame for the ordering is also taken as the molecular (x', y', z') frame. The order parameter of the

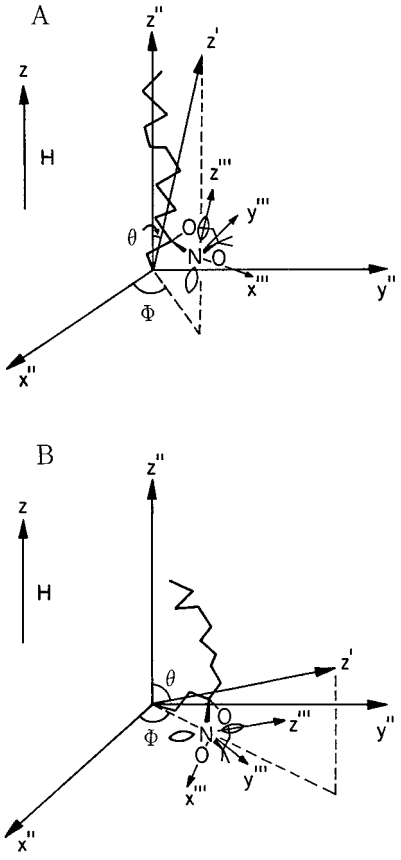

FIGURE 1 Axis frames used in the spectral simulations: the molecular frame (x', y', z'), the local director frame (x'', y'', z'') (only the z'' axis is shown), the magnetic frame (x''', y''', z'''), and the laboratory frame (x, y, z) (only the z axis is shown, which is parallel to the magnetic field H). (*A*) A nitroxide radical is attached to the end chain segment in the *trans* conformation preferentially oriented along the z'' axis. The nitroxide radical has a positive order parameter. (*B*) A nitroxide radical is attached to a bent end chain segment in the *trans* conformation. The nitroxide radical has a negative order parameter. Note that in both (*A*) and (*B*) z' is parallel to z''', and x' and y' (not shown) can be taken parallel to x''' and y''', respectively. Also, in both (*A*) and (*B*) the angle of tilt Ψ between the z'' and z axes is taken as 0°.

spin label, *S*, is defined as follows:

$$S \equiv \langle D^2_{00} \rangle = \left\langle \frac{1}{2}(3\cos^2\theta - 1) \right\rangle = \int d\Omega D^2_{00}(\Omega) P(\Omega).$$

It is a measure of the extent of alignment of the z' molecular axis with respect to the z'' local director frame. In a similar manner we define the nonaxial order parameter

$$S_2 \equiv \langle D^2_{02} + D^2_{0-2} \rangle = \langle \sqrt{3/2} \sin^2\theta \cos 2\phi \rangle,$$

which measures the extent to which there is a preferential alignment of the molecular x' vs. y' axis with respect to the z'' axis. $P(\Omega)$, the orientational probability distribution, is given by

$$P(\Omega) = \frac{\exp(-U(\Omega)/kT)}{\int d\Omega \exp(-U(\Omega)/kT)} \qquad (2)$$

where k is Boltzmann's constant, T is the temperature, and $U(\Omega)$ is an ordering potential experienced by the nitroxide moiety, which can be approximated as

$$-U(\theta, \phi)/kT = \frac{\epsilon_0^2}{2}(3\cos^2\theta - 1) + \sqrt{\frac{3}{2}}\epsilon_2^2 \sin^2\theta \cos 2\phi \qquad (3)$$

where $\Omega \equiv (\theta, \phi)$, and the angles θ and ϕ represent polar and azimuthal angles of the diffusion axis z' in the local director frame. The ϵ_0^2 and ϵ_2^2 are dimensionless potential energy coefficients. The magnetic frame (x''', y''', z''') is the axis frame in which the *g*-tensor and *A*-tensor are diagonalized. By convention, the x''' axis points along the N–O bond, the z''' axis is parallel to the $2p_z$ axis of the nitrogen atom, and the y''' axis is perpendicular to the others, forming a right-handed coordinate system.

The z'' axis of the local director frame (x'', y'', z'') represents the average orientation of the acyl chains in a lipid bilayer fragment. Because of the axial symmetry of the acyl chain orientation, the x'', y'' axes can be chosen arbitrarily. The fourth axis frame is the laboratory frame (x, y, z), which is defined by the magnetic field, z axis. In Fig. 1, *A* and *B*, only the z axis is shown.

Two tilt angles relevant to this study are defined as follows. A director tilt, Ψ, is the angle a local director (z'' axis) makes with respect to the magnetic field (z axis). In Fig. 1, the z'' axis is parallel to the magnetic field, therefore the director tilt is 0°. The director tilt is related to the macroscopic ordering of the lipid bilayers. A macroscopically aligned lipid sample has a uniform director tilt, which is the angle between normal to the sample plate and the magnetic field. Whereas for lipid vesicles, the director tilt of the bilayer fragment is randomly distributed in space, i.e., macroscopically this lipid sample is disordered. However, locally in each bilayer fragment acyl chains are uniformly oriented, i.e., microscopically this lipid sample is ordered. Therefore, lipid vesicles are said to be microscopically ordered but macroscopically disordered (MOMD) (Meirovitch et al., 1984), as discussed in the Introduction. The second tilt angle, diffusion tilt β, is the angle between the magnetic z''' axis and the molecular z' axis, which is related to the conformation of the chain segment to which the nitroxide radical is attached (Ge and Freed, 1993). For DOXYL-type spin labels, e.g., 16PC, if a segment to which the DOXYL group is attached is in a *trans* conformation, then the molecular and magnetic frames coincide with each other, as shown in Fig. 1, *A* and *B*, i.e., $\beta = 0°$. [Note that Budil et al. (1996) use subscripts of *m*, *R*, *d*, and *L* instead of ‴, ′, ″, and unprimed, respectively.]

RESULTS

Features of the ESR spectra

ESR spectra were taken for DPPC/GA vesicle dispersions of molar ratio 5, 12.5, 15, and 20 at temperatures of 30°, 35°, 37°, 39°, and 40°C in the gel phase, and 41° and 45°C in the liquid crystalline (L_α) phase for both heating and cooling cycles. The heating cycle consisted of initially raising the temperature from room temperature to 30°C, and then taking the spectra at increasing temperature. Then, after the last spectrum was taken at 45°C, the sample was heated to 75°C at a rate of ~3°C/min, and it was annealed at this temperature for 3 min. To begin the cooling cycle, the sample was first cooled down to 45°C at the same rate, and then spectra were taken at decreasing temperatures. The reproducibility was good. It was checked by preparing new samples and then following the same heating and cooling cycles. For dispersions of DPPC/GA ratios of 15, 20, and of pure DPPC, the spectra obtained in heating and cooling cycles are identical, but for dispersions of DPPC/GA ratios

of 12.5 and 5, the spectra from heating and cooling cycles are different. Fig. 2 shows ESR spectra of 16PC in DPPC dispersions for DPPC/GA ratio of 5 (both heating and cooling cycles), and ratio of 15 (heating cycle), and pure DPPC dispersions (heating cycle). In Fig. 2, the simulated spectra from the nonlinear least-squares fit (*dotted lines*) are superimposed on the corresponding experimental spectra (*solid lines*).

We note in Fig. 2 the existence of additional splittings of the outer peaks in spectra from dispersions of DPPC/GA ratio of 5, which are not present in spectra from DPPC/GA ratios of 15 and from pure DPPC. The results for the 12.5 ratio also show the additional splittings, but they are weaker than for a ratio of 5 (data not shown). Also, no additional splittings were found in the spectra from DPPC/GA ratio of 20 (data not shown). The additional peaks in the spectra from DPPC dispersions containing high concentrations of GA (high [GA], i.e., DPPC/GA ratios of 5 and 12.5) will be referred to as arising from "boundary lipids." The peaks in the spectra from dispersions of high [GA] that are similar to those from dispersions of low [GA] (DPPC/GA ratio of 15 and 20) will be referred to as arising from the "bulk lipids." Thus, we have the common observation of the presence of boundary lipids once the GA/DPPC ratio is $>$1:15 (Ge and Freed, 1993 and references therein). As will be discussed below, the lipids represented by the two components are most probably in different phase structures. The bulk lipids are in a lamellar phase that is similar to those containing low [GA] (GA/DPPC $<$1:15), whereas the boundary lipids could be either in a lamellar or an H_{II} phase.

The conventional definition of boundary lipids is those lipids in the immediate vicinity of GA molecules. However, in GA/DPPC dispersions of low [GA], only one component was discernible. Possibly, the differences in spectra from the bulk and boundary lipids in these low [GA] dispersions are not very large, so they cannot be resolved. Therefore, in this paper we simply refer to all the lipids in the low [GA] dispersions and the lipids with similar spectra in the high [GA] dispersions as bulk lipids, with the lipids yielding the additional splitting in the high [GA] dispersions being referred to as boundary lipids. However, one sees from Fig. 2 that the spectra in the heating cycle obtained from high [GA] dispersions are more spread at both wings than the spectra obtained at the same temperature in the cooling cycle. The outer peak separation of the boundary lipid peaks in the 30°C spectrum for a DPPC/GA ratio of 5 obtained in the heating cycle is 64.7 G, which decreases to 60.8 G in the cooling cycle. It can also be seen in Fig. 2 that at temperatures above 30°C the intensities of the outer peaks from the cooling cycle are always weaker than those from the heating cycle. This seems to imply some differences in the boundary lipid phase depending on thermal history.

Quenching is a useful method to study structural relaxation in materials. Usually a material is first heated to a high temperature to allow it to deviate significantly from its normal state. Then the material is quenched to a sufficiently low temperature to freeze the perturbed state in the material. Physical or chemical properties of the material may then be monitored as the material relaxes back to its original unperturbed state. An analysis of the relaxation process can

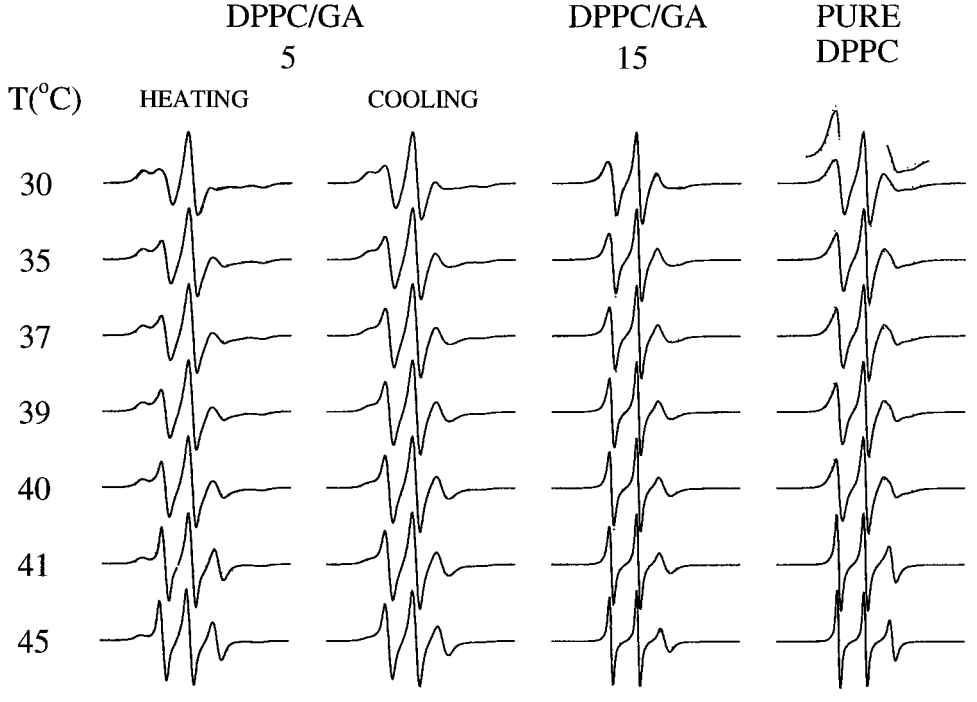

FIGURE 2 ESR spectra of the spin probe 16PC (0.5 mol %) in GA/DPPC dispersions at molar ratios of 5 (heating and cooling cycles) and of 15 (heating cycle), and in pure DPPC dispersions (heating cycle); (—) experimental spectra, (· · ·) simulations. The temperatures are indicated in the figure.

provide structural and dynamical information about the material. Thus, we performed a quenching experiment on GA/DPPC dispersions of ratio 5. Specifically, the dispersions were treated in the following way: annealing at 75°C for 30 min; cooling down to room temperature; annealing at 75°C again for 10 min; then quenching in ice water (such samples are referred to as quenched samples). The spectra were taken in both heating and cooling cycles in the same manner as for unquenched samples. The spectra from both cycles were found to be identical. These spectra are similar to but not exactly the same as those from the unquenched sample with the same DPPC/GA ratio in the cooling cycle. The outer peak separation at 30°C is 62.1 G for the quenched sample, which is between the values for the heating and cooling cycles at 30°C from the unquenched sample. The intensities of the boundary lipid peaks in the spectra from the quenched sample are weaker than those from unquenched samples in the cooling cycle. After the quenched sample was stored in a refrigerator for 2½ months, it was found that its ESR spectrum changed significantly (spectrum not shown), i.e., the outer peak separation increased to 62.7 G.

Simulations and comparison with the 2D-FT-ESR study

The latest version of the NLLS fitting program for slow-motion ESR was employed (Budil et al., 1996). It enables one to fit the ordering and dynamic parameters and the weights of the component spectra. In our efforts at fitting the spectra, we were concerned with possible ambiguities in fitting the limited resolution MOMD spectra from the vesicles, as discussed in the Introduction, and we wished to benefit from the results of the recent 2D-FT-ESR study (Patyal et al., 1997) on the effect of GA (in a 1:5 ratio with DPPC) on the bulk lipid, as also discussed in the Introduction. Initially we sought to achieve the best NLLS fits obtainable with the programs for simple but reasonable models. Whereas it was clearly necessary to fit the experimental spectra from DPPC vesicles containing high [GA] with two components, (i.e., bulk and boundary lipids), to reproduce the observed spectra peaks, the spectra from vesicles containing low [GA] could be reasonably simulated with just a single component, (i.e., just bulk lipid). These spectra were qualitatively similar to those from vesicles from just pure DPPC. Actually, the quality of the two-component fits of the spectra from molar ratios 5 and 12.5 is better in the details than the one-component fits in the other cases, especially for the gel phase. This is clearest for the case of pure DPPC (Fig. 2). Detailed features in the high field region of the spectra in the gel phase are indicative of the presence of two components. The more subtle features are quite different from the prominent features observed with the high [GA]. It was possible to improve these fits by using two components, although we found there is uncertainty about the uniqueness of the fits and the details of the models. Because of these uncertainties we chose to use the simpler fits to just one component for the pure DPPC and for molar ratios of 15 and 20 of DPPC to GA.

In the simulations of Patyal et al. (1997) of their 2D-FT-ESR spectra, they found that a diffusion tilt angle (i.e., the angle between the z' and z''' axes, cf. Fig. 1) of $\beta \approx 31°$ led to the best fits, which was important in their ability to fit their lower temperature results. Although they performed separate fits with $\beta = 0°$ and $\beta = 31°$ for comparison, the results for $\beta = 31°$ were reported. (Patyal et al. do point out that the improved fits achieved with $\beta = 31°$ are probably indicative of the limitations of the model, e.g., it would be necessary to consider both internal modes of motion and the overall motion). In the same spirit, we fit representative cw-ESR spectra with $\beta = 0°$ and $\beta = 31°$. We found that the cw-ESR spectra are better fit with $\beta = 0°$, especially in the gel phase, so we chose to consistently use this value for β in our present fits. The main ordering and dynamic parameters obtained in this manner from NLLS fits to our cw-ESR spectra for GA/DPPC molar ratios of 1:5 and 1:12.5 (heating and cooling cycles), and pure DPPC are presented in Tables 1–5. As in previous work (Kar et al., 1985; Shin and Freed, 1989), we find that the results are insensitive to the value of $R_\parallel$, since $R_\parallel > R_\perp$, so we do not list the $R_\parallel$. We also compare, where available, with the results obtained from the 2D-FT-ESR study (Patyal et al., 1997). That study for a molar ratio of 5 corresponded better to the present results obtained in the cooling cycle. Thus, in Table 2, for this case, we provide the results for the bulk lipid obtained from the 2D-FT-ESR study for the case of $\beta = 0°$, for 45°C (L_α) phase and for 35°C (gel phase). For 45°C, results are shown for both the S_{c-} 2D spectrum (which are more resolved, due to echo-like cancellation of inhomogeneities) and the S_{c+} 2D spectrum (which are less resolved, since they lack the echo-like cancellation). They are quite similar. Rather good agreement for $R\perp$ and ϵ_0^2 is obtained between the results of the cw-ESR and the 2D-FT-ESR experiments. For 30°C, only the less-resolved S_{c+} spectra could be fit with $\beta = 0°$, so these values are shown. Again, reasonable agreement is achieved for the bulk lipid in the 5:1 DPPC/GA mixtures. This is not quite the case for the results from pure DPPC vesicles, as seen from Table 5.

For the pure DPPC vesicles, we provide in Table 5 both the S_{c+} and S_{c-} results with $\beta = 0°$ for 45°C and the S_{c+} result with $\beta = 0°$ for 35°C. Here the cw-ESR values of $R_\perp$ are about a factor of 2 smaller than those from 2D-FT-ESR, while the values of ϵ_0^2 are substantially larger. A likely explanation could be the following. As we noted above, the cw-ESR spectra, especially in the gel phase, for the pure DPPC vesicles clearly show the presence of two components. Their superposition would necessarily lead to extra IB, which is attributed, in the single-component fits, partly to increased HB and partly to increased IB due to an enlarged MOMD effect resulting from increased ordering. Whereas the two-component fitting to these spectra is not unique (see above), reasonable fits can be found in which there is a faster motional component with parameters sim-

TABLE 1 Parameters obtained from nonlinear least-squares fitting of ESR spectra of 16PC in vesicles of DPPC/GA ratio of 5 (heating cycle)

Temp. (°C)	Component	$R_\perp$ (s^{-1})	ϵ_0^2	ϵ_2^2	S	S_2	Population*
30	1#	5.76×10^6	−6.14	−0.88	−0.42	−0.53	0.42
	2§	6.92×10^7	1.91	−1.76	0.28	−0.33	0.58
35	1	1.35×10^7	−7.60	−1.24	−0.44	−0.69	0.48
	2	1.00×10^8	0.97	−0.77	0.18	−0.22	0.52
37	1	1.44×10^7	−7.55	−1.29	−0.44	−0.70	0.48
	2	1.08×10^8	0.94	−0.75	0.17	−0.21	0.52
39	1	1.53×10^7	−7.62	−1.09	−0.44	−0.63	0.45
	2	1.09×10^8	0.75	−0.52	0.15	−0.16	0.55
40	1	1.70×10^7	−7.82	−1.05	−0.44	−0.62	0.44
	2	1.29×10^8	0.61	−0.50	0.12	−0.16	0.56
41	1	1.66×10^7	−6.80	−0.37	−0.43	−0.25	0.21
	2	2.00×10^8	0.43	−0.40	0.08	−0.14	0.79
45	1	2.04×10^7	−5.01	−0.42	−0.40	−0.28	0.46
	2	2.04×10^8	0.53	−0.69	0.09	−0.23	0.54

A-tensor components are $A_{xx} = A_{yy} = 5.0$ G, $A_{zz} = 33.7$ G (Ge and Freed, 1993); *g*-tensor components are $g_{xx} = 2.0089$, $g_{yy} = 2.0058$, $g_{zz} = 2.0021$ (Tanaka and Freed, 1985). The least-squares estimated errors in $R_\perp$, ±5%; in ϵ_0^2, ≤0.1; in ϵ_2^2, ≤0.05.

*The average population of boundary lipid (component 1) is 43.8%.

#1, boundary lipid.

§2, bulk lipid.

ilar to those of Patyal et al. shown in Table 5, and a significantly slower (by a factor of 2–3) component with different ordering characteristics. This slower motional component would be significantly suppressed in the 2D-FT-ESR spectrum due to its faster decay during the spectrometer dead time by virtue of its shorter T_2 (cf. Patyal et al., 1997). Thus, the faster motional component is heavily favored (or weighted) in the 2D-FT-ESR experiment. More generally, we can recognize that when there are (similar) components present in an ESR spectrum, the cw-ESR and 2D-FT-ESR will weight them differently. Given these uncertainties in the interpretation of the cw-ESR spectra, especially those containing lower (or no) GA, we will primarily emphasize the trends in the different spectra and their fits in our exploration of the aggregation of GA and its effects on membrane structure and dynamics.

Let us first consider the cases of larger GA concentration (e.g., 1:5) for which the fits for the bulk lipid component are in reasonable agreement with the 2D-FT-ESR. In Fig. 3 we show the spectra for the two components corresponding to

TABLE 2 Parameters obtained from nonlinear least-squares fitting of ESR spectra of 16PC in vesicles of DPPC/GA ratio of 5 (cooling cycle)

Temp. (°C)	Component	$R_\perp$ (s^{-1})	ϵ_0^2	ϵ_2^2	S	S_2	Population*
30	1#	1.76×10^7	−4.58	−0.28	−0.39	−0.18	0.47
	2§	1.04×10^8	1.72	−1.67	0.25	−0.34	0.53
35	1	1.95×10^7	−4.88	−0.17	−0.40	−0.11	0.36
	2	1.14×10^8	1.06	−0.87	0.19	−0.23	0.64
		$(0.98 \times 10^8$	0.59	−0.13	0.12	−0.04)¶	
37	1	2.14×10^7	−4.50	−0.21	−0.39	−0.14	0.33
	3	1.30×10^8	1.00	−0.93	0.17	−0.26	0.67
39	1	2.40×10^7	−4.95	−0.20	−0.40	−0.13	0.33
	2	1.40×10^8	0.81	−0.65	0.15	−0.20	0.67
40	1	2.78×10^7	−4.31	−0.04	−0.38	0.01	0.35
	2	1.80×10^8	0.83	−0.72	0.15	−0.21	0.65
41	1	3.24×10^7	−4.44	−0.04	−0.39	−0.03	0.42
	2	2.06×10^8	0.83	−0.69	0.15	−0.21	0.58
45	1	3.24×10^7	−4.77	−0.20	−0.40	−0.13	0.30
	2	2.21×10^8	0.58	−0.52	0.11	−0.17	0.70
		$(1.89 \times 10^8$	0.64	0.12	0.14	0.03)‖	
		$(2.32 \times 10^8$	0.31	0.19	0.06	0.07)¶	

Values for bulk lipid from 2D-FT-ESR (Patyal et al., 1997) are in parentheses. They correspond to fits with $\beta = 0°$. See Table 1 for tensor components and least-squares estimated errors.

*The average population of boundary lipid (component 1) is 36.4%.

#1, boundary lipid.

§2, bulk lipid.

¶Results from S_{c+} spectra.

‖Results from S_{c-} spectra.

TABLE 3 Parameters obtained from nonlinear least-squares fitting of ESR spectra of 16PC in vesicles of DPPC/GA = 12.5 (heating cycle)

Temp. (°C)	Component	$R_\perp$ (s^{-1})	ϵ_0^2	ϵ_2^2	S	S_2	Population*
30	1#	9.59×10^6	−5.29	−0.53	−0.41	−0.34	0.33
	2§	9.08×10^7	1.35	−0.91	0.25	−0.22	0.67
35	1	1.70×10^7	−4.18	−0.48	−0.38	−0.30	0.34
	2	1.06×10^8	0.85	−0.41	0.18	−0.12	0.66
37	1	1.90×10^7	−5.87	0.65	−0.42	0.41	0.37
	2	9.84×10^7	0.68	0.15	0.15	0.05	0.63
39	1	2.71×10^7	−5.58	0.52	−0.41	0.34	0.37
	2	1.17×10^8	0.59	0.03	0.13	0.01	0.63
40	1	3.16×10^7	−3.21	1.41	−0.37	0.69	0.33
	2	1.38×10^8	0.54	−0.20	0.11	0.07	0.67
41	1	3.55×10^7	−1.05	−0.22	−0.18	−0.11	0.31
	2	2.14×10^8	0.58	−0.51	0.11	−0.17	0.69
45	1	6.30×10^7	−0.92	−0.07	−0.16	−0.03	0.33
	2	2.75×10^8	0.44	−0.39	0.08	−0.13	0.67

See Table 1 for tensor components and least-squares estimated errors.
*The average population of boundary lipid (component 1) is 33.7%.
#1, boundary lipid.
§2, bulk lipid.

the bulk and boundary lipids that are obtained from the NLLS fit for the case of DPPC/GA molar ratio of 5 for the heating cycle at 30°C. They are superimposed on the experimental spectrum. It can be seen that the two outer peaks of the boundary lipid component are widely spread. This component is characterized by having an $R_\perp$ that is one order of magnitude smaller than that for the bulk lipid (cf. Table 1). This result is true for all temperatures as well as for the heating and cooling cycles (cf. Tables 1 and 2). The boundary lipid exhibits substantially greater ordering, but the ordering is *negative*. We discuss the implication of this negative ordering below. These features are also true for all temperatures as well as for the heating and cooling cycles (cf. Tables 1 and 2). In addition, very similar conclusions emerge for the case of a molar ratio for DPPC/GA of 12.5. The average fraction (over temperature) for the boundary lipid is 0.44 (heating cycle) and 0.36 (cooling) for DPPC/GA = 5, and 0.34 (heating) and 0.20 (cooling) for DPPC/GA = 12.5. This accounts for the larger intensities of the boundary lipid component in the heating cycle than in the cooling cycle, and it also shows that the amount of the boundary lipid increases with the content of GA.

Patyal et al. (1997) concluded from their 2D-FT-ESR spectra that a boundary lipid characterized by an $R_\perp$ in the range $2 \times 10^6 \leq R_\perp \leq 6 \times 10^7$ s^{-1} (at 45°C) *and* low ordering ($S < 0.1$) "would most likely not be observable in the experimental (2D) spectra." The value of $R_\perp = 3.2 \times 10^7$ s^{-1} from Table 2 is consistent with this. Patyal et al. did not consider the possibility of a large (negative) order parameter ($S = -0.4$) as well. We have repeated the 2D-FT-ESR simulations using the 45°C parameters listed in Table 2, and we have confirmed that they are indeed con-

TABLE 4 Parameters obtained from nonlinear least-squares fitting of ESR spectra of 16PC in vesicles of DPPC/GA = 12.5 (cooling cycle)

Temp. (°C)	Component	$R_\perp$ (s^{-1})	ϵ_0^2	ϵ_2^2	S	S_2	Population*
30	1#	1.86×10^7	−2.55	−0.34	−0.32	−0.20	0.29
	2§	1.15×10^8	1.55	−1.24	0.27	−0.27	0.71
35	1	1.90×10^7	−2.36	−0.34	−0.30	−0.20	0.19
	2	1.03×10^8	0.98	−0.57	0.20	−0.16	0.81
37	1	2.82×10^7	−2.18	−0.32	−0.29	−0.18	0.23
	2	1.18×10^8	0.88	−0.56	0.17	−0.16	0.77
39	1	4.07×10^7	−2.43	−0.57	−0.31	−0.32	0.19
	2	1.25×10^8	0.70	−0.55	0.13	−0.17	0.81
40	1	4.47×10^7	−1.91	−0.45	−0.27	−0.24	0.22
	2	1.43×10^8	0.68	−0.58	0.13	−0.18	0.78
41	1	4.52×10^7	−2.42	−0.65	−0.31	−0.37	0.18
	2	1.55×10^8	0.61	−0.56	0.11	−0.18	0.82
45	1	4.51×10^7	−2.52	−0.61	−0.32	−0.34	0.15
	2	2.51×10^8	0.59	−0.57	0.11	−0.19	0.85

See Table 1 for tensor components and least-squares estimated errors.
*The average population of boundary lipid (component 1) is 20.0%.
#1, boundary lipid.
§2, bulk lipid.

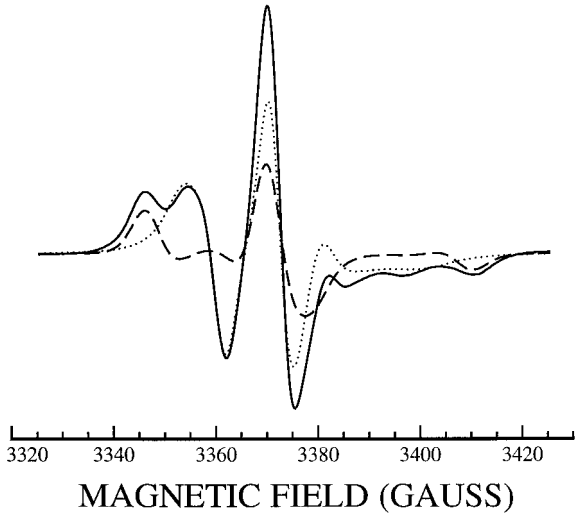

FIGURE 3 Two components, corresponding to the bulk (· · ·) and boundary (− − −) lipids obtained from the NLLS fit for the ESR spectrum of 16PC in GA/DPPC dispersions of molar ratio 5 for the heating cycle at 30°C, are superimposed on the experimental spectrum (—).

sistent with the statement quoted from Patyal et al. That is, the 2D spectra are virtually completely dominated by the fast component, i.e., the bulk lipid. However, very subtle features in the wings of the auto-peaks might be discernible with a sufficient signal-to-noise ratio. A reexamination of the experimental 2D spectra has shown that features of this type might well be present, but further work would be needed to confirm it. Thus, the fits to the boundary lipid component we obtained are not unreasonable, and they show consistent trends over variations in temperature, composition, and heating versus cooling cycles.

We also addressed the question of uniqueness of our fits that lead to the negative order parameter for the boundary lipid by repeating the least-squares fits with a wide range of different seed values of the parameters. In nearly all cases the convergence was to the results in Tables 1 and 2 within the uncertainty of the simulation. However, it was found that if a large positive order was used for the seed values, it is possible to obtain a reasonably good fit with large positive order parameters (~0.8) and slow motion. This is clearly a less robust solution suggestive of a local minimum. A close examination showed that this fit is not entirely satisfactory, in that the outer wings of the spectrum are not very well fit. In particular, the outer peak separation of the simulation is smaller than that of the experimental spectrum, whereas in the negative ordering fit, they match with each other very well. Also, the fits obtained for the bulk lipid are a little less consistent with the 2D-ELDOR results. In addition, the high positive ordering at high [GA] is not consistent with the well-known observations that high [GA] increases the disorder of the lipid, as we discuss below.

Significance of a negative order parameter: a dynamic bending of end acyl chains

A key feature of the spectral component attributed to boundary lipid is its large outer peak separation. It is 64.7 G at 30°C for a DPPC/GA ratio of 5, which is close to the outer peak separation of the rigid limit spectrum at −146°C, i.e., 67.4 G. The key feature of our analysis of this spectrum is the large negative order parameter. The best way to understand the significance of a negative order parameter of the acyl chain is to compare the orienting potentials along three specific directions: $(\theta, \phi) = (90°, 0°), (90°, 90°), (0°, 0°)$, which specifies the orientations of the x', y', and then the z' axis being parallel to the z'' axis, respectively (see Fig. 1 *B* and associated legend). One can easily verify from the symmetry of Eq. 2 that the minimum of the orienting potential $U(\theta, \phi)$ must always lie along one of the three directions. We obtained the potential coefficients from the simulation of the spectrum of 16PC in GA/DPPC dispersions of ratio 1:5 at 30°C in the heating cycle for the boundary lipid, $\epsilon_0^2 = -6.14$, $\epsilon_2^2 = 0.42$, and for the bulk lipid, $\epsilon_0^2 = 1.91$, $\epsilon_2^2 = -1.76$. The corresponding orienting potentials for the boundary lipid using Eq. 3 are $u_x \equiv U(90°, 0°)/kT = -2.00$, $u_y \equiv U(90°, 90°)/kT = -4.14$, and $u_z \equiv U(0°, 0°)/kT = 6.14$. This shows that in the boundary lipid there is a strong preference for the y' axis, a less strong

TABLE 5 Parameters obtained from nonlinear least-squares fitting of ESR spectra of 16PC in vesicles of DPPC

Temp. (°C)	$R_\perp$ (s^{-1})	ϵ_0^2	ϵ_2^2	S	S_2
30	6.31×10^7	1.52	2.11	0.13	0.47
35	7.91×10^7	1.33	2.18	0.07	0.52
	$(1.69 \times 10^8$	0.39	0.73	0.05	0.25)*
37	8.51×10^7	1.37	2.29	0.06	0.54
39	8.91×10^7	1.29	2.21	0.06	0.53
40	8.92×10^7	1.26	2.19	0.06	0.53
41	1.41×10^8	0.82	−1.91	0.002	0.53
45	2.14×10^8	0.74	−1.78	0.005	0.51
	$(4.20 \times 10^8$	0.43	0	0.09	0)#
	$(3.80 \times 10^8$	0.25	0	0.05	0)*

The *A*-tensor components are $A_{xx} = A_{yy} = 4.9$ G, $A_{zz} = 33.0$ G (Ge and Freed, 1993); see Table 1 for *g*-tensor components and least-squares estimated errors. Values from 2D-FT-ESR (Patyal et al., 1997) are in parentheses. They correspond to fits with $\beta = 0°$.

*Indicates results from S_{c+} spectra.

#Indicates results from S_{c-} spectra.

preference for the x' axis, and a strong negative preference preventing the z' axis of the nitroxide radical moiety to align along the z'' axis (the normal to the bilayer surface). In other words, there is a strong tendency for the z' axis to align perpendicular to the z'' axis (cf. Fig. 1 *B*). For comparison, the corresponding orienting potentials for the bulk lipid are $u_x = 3.10$, $u_y = -1.19$, and $u_z = -1.91$. This shows that the z' axis of the nitroxide radical moiety in the bulk lipid is preferentially oriented along the z'' axis, the local director of the bilayers (cf. Fig. 1 *A*).

The above analysis of orienting potentials can be visualized by a plot of the orientational distribution function (Eq. 2) for the bulk and the boundary 16PC lipids, which is shown in Fig. 4. In terms of the language of ESR spectral simulations, it is said that the nitroxide radical is z-ordered in the bulk lipid and y-ordered in the boundary lipid. This corresponds to a dynamic bending of the end chain in the boundary lipid toward the middle surface of the bilayer. By dynamic bending we mean that an end chain segment, while undergoing rotational diffusion, is usually oriented such that its symmetry axis (the z' axis) points in a direction perpendicular to the z'' axis (cf. Fig. 1 *B*). This would necessarily correspond to the z' symmetry axis of the nitroxide moiety being randomly distributed in the x''-y'' local membrane vesicle plane, consistent with disorder observed in the lipid chain by other techniques (Rice and Oldfield, 1979; Lee et al., 1984; Cortijo et al., 1982; Short et al., 1987; Cornell et al., 1988) due to high [GA].

As will be argued below, the dynamic bending of the end chain segment is caused by a shrinkage of the acyl chain in the GA/lipid dispersions at high [GA], which is commonly described as a disordering of the acyl chain. However, this is different from the disordering resulting from a nearly uniform distribution of orientations of the chain segment, such as in the case of the end chain segment in the liquid crystalline phase characterized by a nearly zero order parameter of 16PC in pure DPPC at 45°C (see Table 5).

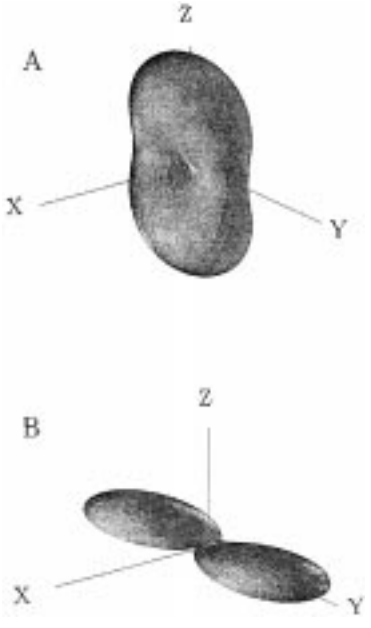

FIGURE 4 A 3D plot of the orientational probability distribution, $P(\Omega)$ (see Eq. 2) for 16PC in GA/DPPC dispersions of molar ratio 1:5 at 30°C in the heating cycle. (*A*) Bulk lipid, with $\epsilon_0^2 = 1.91$, $\epsilon_2^2 = -1.76$. (*B*) Boundary lipid, with $\epsilon_0^2 = -6.14$, $\epsilon_2^2 = -0.88$.

Thus, there are two special features for the boundary lipid: the negative order parameter and the large outer peak separation. In fact, the two features are closely related. This arises from two considerations. First, in calculating a MOMD spectrum, the spectra from all orientations are integrated with weight $\sin\Psi d\Psi$ for orientations between Ψ and $\Psi + d\Psi$. Thus orientations for which $\Psi \approx 90°$ are heavily weighted, while those for $\Psi \approx 0°$ are very weakly weighted. For a fully extended 16PC with $\Psi = 0°$, the z''' axis (parallel to the z' axis) will be parallel to B_o, so the *A*-tensor component A_{zz}, which is the largest component for 16PC, will make a small contribution to the integral. For $\Psi = 90°$, the smaller A_{xx} and/or A_{yy} are parallel to B_o. A positive order parameter, *S*, would guarantee a preferential alignment of the acyl chain, to which the nitroxide is attached, to be parallel (perpendicular) to B_o for $\Psi = 0°$ ($\Psi = 90°$). However, a negative *S* implies that the end of the acyl chain prefers to be perpendicular to the main chain axis, i.e., the end of the chain prefers to be bent. Thus for $\Psi = 0°$, the z''' axis will prefer to be perpendicular to B_o, whereas for $\Psi = 90°$, the z''' axis can be favorably aligned with respect to B_o. This leads to MOMD spectra with large outer peak splittings, consistent with the observations.

An x-ray diffraction study of single crystals of DPPC and GA showed that the lipid chains are interdigitated (Wallace and Janes, 1991). A discussion in our previous work (Ge and Freed, 1993) about differences in the acyl chain structure between lipid/protein/water dispersions and lipid/protein crystals led to the suggestion that the water entering the lipid/GA interface (water penetration) might be responsible for the disordering effect of high [GA]; thus the boundary lipids are most likely to be disordered. Our current analysis indicates that the disordering effect at high [GA] stems from the bending of chain ends of boundary lipids. This implies that the lipid chain structure in the hydrated and anhydrous lipid/protein systems are quite different. In fact, Killian and de Kruijff (1985b) showed that just by varying the water content, different lipid phase structures result within the same DOPC/GA/water system.

Ordering effect of GA at low [GA]

Fig. 5 shows that at all temperatures studied, the order parameter S of the bulk lipids increases with [GA] up to the GA/DPPC ratio around 1:15, and upon further increasing [GA] it levels off. We (Ge and Freed, 1993; Table 1) previously found that GA increases water penetration into the hydrophobic core of DPPC bilayers, which was revealed by increases in A_{zz} of spin labels 10PC and 16PC in GA/

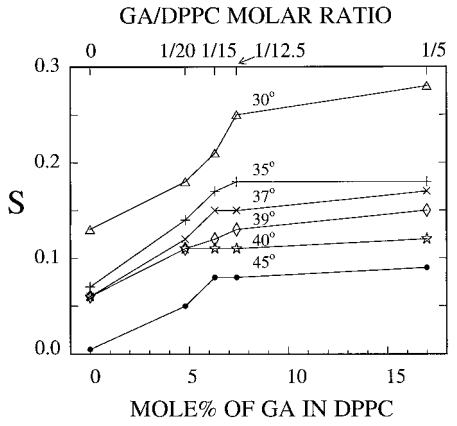

FIGURE 5 Variations of order parameters (*S*) of the bulk lipids with the concentration of GA in DPPC dispersions at various temperatures, as indicated in the figure.

DPPC dispersions. This was even more dramatically demonstrated by the variations in g_{xx} seen for these and other chain PCs in ESR experiments at 250 GHz (Earle et al., 1994). This effect also increases with [GA] and levels off near a GA/DPPC molar ratio of 1:15. These observations and the emergence of boundary lipid at GA/DPPC ratios ~1:15 are in agreement with the aggregation of GA molecules, which was first suggested by Chapman et al. (1977). This suggestion was supported by the observation that the deuterium quadrupole splitting of a specifically labeled DMPC increases linearly with [GA] at DMPC/GA ratios of >15, but decreases slowly at ratios of <15 (Rice and Oldfield, 1979).

Hysteresis in cooling cycle versus in the heating cycle

In addition to the fact that there is a greater fraction of boundary lipid for the heating than the cooling cycle, there are other indications of hysteresis. That is, there are differences in the spectra of 16PC between the heating and cooling cycles for the lower DPPC/GA ratios of 5 and 12.5 (i.e., high [GA]) that are reflected in the enhanced $R_\perp$ for both boundary and bulk lipids in the cooling cycle versus the heating cycle, (cf. Figs. 6, *A* and *B* and 7, *A* and *B*). Such hysteresis effects are shown more clearly for the DPPC/GA ratio of 5 than 12.5. Hysteresis effects can also be seen from the decrease in magnitude of ordering of the boundary lipids in the cooling versus heating cycles at the high [GA], (Fig. 8, *top*). However, the variation in order parameter of the bulk lipids with temperature shows little hysteresis, (cf. Figs. 6 *C* and 7 *C*). (Note that our analysis, which is based on single components for boundary and bulk lipid, would be modified if there were, for example, a range of types of boundary lipid present, but our present resolution allows a satisfactory fit with just single components).

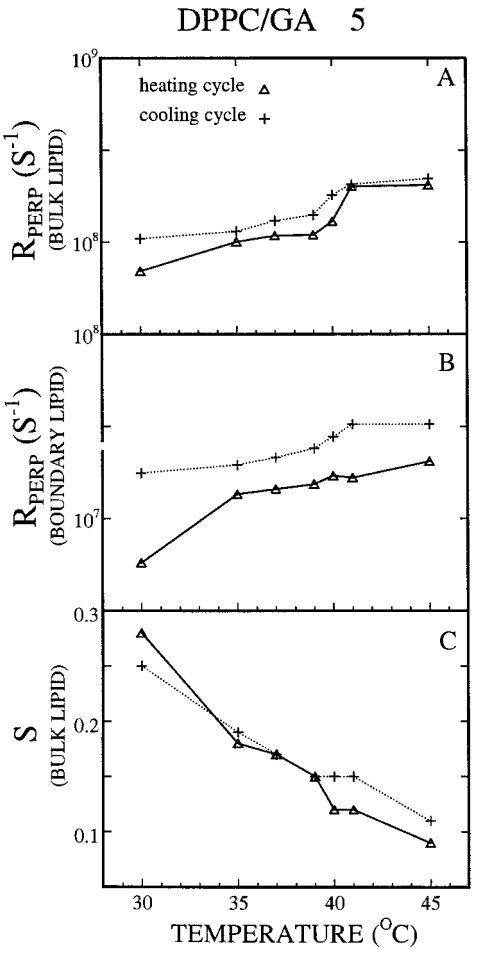

FIGURE 6 Plot of $R_\perp$ of 16PC in bulk (*A*) and boundary (*B*) lipids and of *S* of 16PC in bulk lipid (*C*) for a dispersion of DPPC/GA molar ratio 5 versus the temperature (heating and cooling).

DISCUSSION

Positive or negative hydrophobic mismatch

Hydrophobic mismatch in GA-containing lipid bilayers has attracted much interest (Fattal and Ben-Shaul, 1993; Helfrich and Jakobsson, 1990). Our NLLS spectral fits are consistent with a large negative order parameter for the boundary lipids in DPPC/GA vesicles with high [GA], and this would result from dynamic bending at the end of the acyl chain. That is, our results indicate that the end chain segments are preferentially oriented nearly parallel to the bilayer middle surface. This result is consistent with the existence of hydrophobic mismatch between the GA molecules and the DPPC bilayers, i.e., the hydrophobic length of the GA channel is shorter than the thickness of the acyl chain region (see below). This case was referred to as a "negative hydrophobic mismatch" by Fattal and Ben-Shaul (1993). Our explanation seems consistent with the recent observation using AFM that GA aggregates on a supported DPPC bilayer appear as surface depressions (dark regions) in the bilayer (Mou et al., 1996), but appears to be inconsistent with Watnick et al., (1990). The observations of

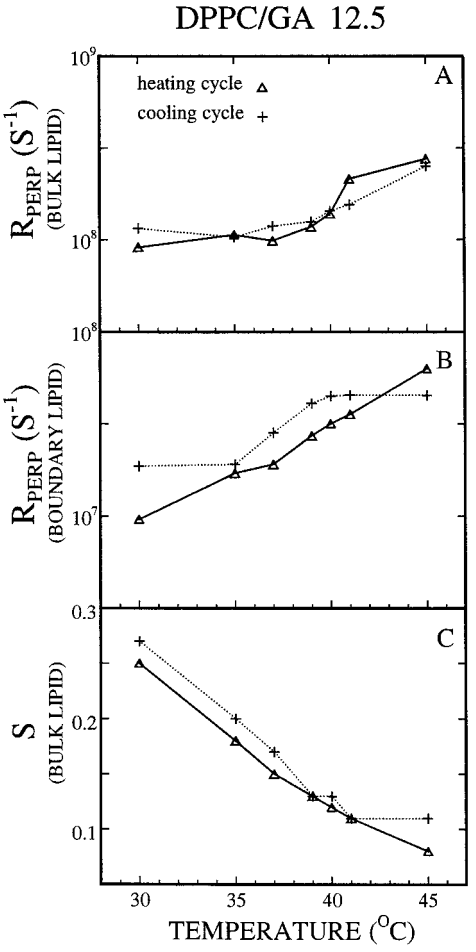

FIGURE 7 Plot of $R_\perp$ of 16PC in bulk (*A*) and boundary (*B*) lipids and of *S* of 16PC in bulk lipid (*C*) for a dispersion of DPPC/GA molar ratio 12.5 versus the temperature (heating and cooling).

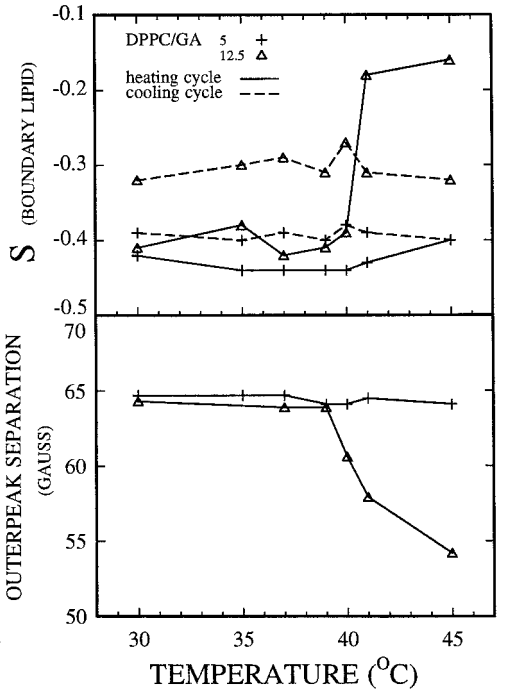

FIGURE 8 *Top:* Plot of *S* of 16PC in boundary lipid for dispersions of DPPC/GA molar ratios 5 and 12.5 versus the temperature (heating and cooling cycles). *Bottom:* Plot of outer peak separations of ESR spectra of 16PC in dispersions of DPPC/GA molar ratios 5 and 12.5 (heating cycles) versus the temperature.

Watnick et al. of a variation of ^{2}H quadrupolar splitting of acyl chains of DPPC with [GA] were similar to those for DMPC reported by Rice and Oldfield (1979). However, they ascribed an initial increase in acyl chain ordering of DPPC at low [GA] to a "positive hydrophobic mismatch," i.e., the hydrophobic length of GA is longer than that of DPPC. This explanation raises a question as to what mechanism is responsible for the increase in the acyl chain ordering at low [GA].

In another context, it was suggested that GA dehydrates the lipid bilayers (Killian and De Kruijff, 1985b), and this plays a role in the lipid H_{II} phase formation (Killian and De Kruijff, 1985b, 1988; Killian et al., 1986; 1987). It remains to be explained how the dehydration effect of GA is related to the dissociation of GA channels, which is a necessary step for the H_{II} phase formation (see Introduction). We suggest an explanation for how the dehydration effect of GA and the hydrophobic mismatch between GA channel and lipid bilayers lead to GA channel dissociation and GA/lipid reorganization, including GA aggregation, and at the same time, it provides an explanation for the apparent contradiction between our ESR results and the AFM results on the one hand with the NMR work of Watnick et al. on the other.

Effects of dehydration by GA on the lipid bilayer structure

Our suggestion is that the ordering effect of low [GA] originates from the dehydration effect of GA, which we first describe. It was observed that swelling of lipids in buffer is strongly reduced upon increasing [GA]. At a GA/lipid ratio $>\sim$1:10, the lipids no longer disperse (de Kruijff et al., 1985). We have made the same observations in our sample preparations. DPPC dispersions hydrated in 100% humidity overnight have properties like a wax, whereas GA/DPPC dispersions of molar ratio 1:5 hydrated under the same condition are like a dried powder. A dried film of the latter sample behaves like a polyester film, i.e., when dipped in water it remains transparent and no swelling is observed. This behavior is usually explained by the observation that GA dehydrates the headgroup region of lipid bilayers by a preferential uptake of water by the GA channel (Killian and de Kruijff, 1985b).

Since we are mainly concerned about the effect of dehydration on the lipid bilayer structure, we suggest that changes in the bilayer structure induced by dehydration are quite similar for the following two processes: incorporating GA into bilayers and dissolving water soluble polymers, such as PEG and dextran, into the aqueous phase of lipid

dispersions. In the latter case, the polymers cannot penetrate into the bilayers, but they do compete for water with lipid headgroups presumably by lowering the free energy of the water, thereby dehydrating the lipid bilayers (Parsegian et al., 1979; Rand and Parsegian, 1989; McIntosh and Simon, 1994; Boni et al., 1984). As a result, lipid bilayers are compressed laterally and stretched longitudinally. The thickness of the water layer decreases, whereas the thickness of the acyl chain region increases; thus the acyl chain ordering increases (Parsegian et al., 1979). We suggest the same changes occur in the bilayer structure for the GA/lipid dispersions. This would explain why the ordering of lipid acyl chains in GA/lipid vesicles increases with [GA] at low [GA].

Thus we expect that all the lipids in the lamellar phase are dehydrated by GA or by the polymers. For GA/lipid systems, this is demonstrated by a significant increase in the ordering of acyl chains of whole bilayers with [GA] at GA/lipid ratios $<$1:15, as mentioned above. Even 2 mol % of GA (GA/lipid ratio $\sim$1:50) increases the deuterium quadrupolar splitting of acyl chains of DMPC bilayers by 7.7% (from 26 kHz for pure DMPC to 28 kHz for 2 mol % GA; Watnick et al., 1990). [Recently, a Monte Carlo study showed that in GA/PC systems the boundary lipid order parameter is rather similar to that of the bulk lipid (Xing and Scott, 1992). A possible reason for this result is that no lipid headgroups were included in their simulations (Xing and Scott, 1992), i.e., the dehydration effect of GA on PC bilayers was not considered.]

Comparison of ordering effect by GA and by cholesterol

It is well known that Chol also increases the acyl chain ordering (for reviews, see Yeagle, 1985; Freed, 1994). However, the mechanism of the ordering effect of Chol must be different from that of GA, because GA dehydrates lipid headgroups, but Chol increases the hydration of headgroups (Ladbrooke et al., 1968). Moreover, GA increases the water penetration into the bilayers (Ge and Freed, 1993; Earle et al., 1994), whereas Chol reduces the water penetration (Simon et al., 1982; Ge and Freed, unpublished results).

Dissociation of GA channels at high [GA]

With the dehydration-induced ordering effect of GA in mind, we can offer an explanation of why high [GA] will lead to the dissociation of GA channels. Suppose for a moment that the hydrophobic length of the pure lipid bilayers matches the length of the exterior hydrophobic surface of the GA channel. Then, after addition of GA, the acyl chain length would increase (due to the dehydration effect), resulting in a negative hydrophobic mismatch; whereas if a negative hydrophobic mismatch exists initially, then it will become more pronounced after addition of GA. Thus, as a consequence of the dehydration effect, the bulk lipids in the bilayers are stretched and subject to tensions along the normal to the bilayer, whereas the boundary lipids surrounding GA channels feel a compression resulting from its tendency to overcome the hydrophobic mismatch with the GA. These two opposing tendencies can be relieved by a dissociation and vertical separation of the two GA monomers. We postulate that there is some limit of [GA] (e.g., GA/DOPC molar ratio of 1:15, see above), at which the stretching force exceeds the strength of the hydrogen bonding between the NH_2 terminals of two GA monomers, enabling the dissociation of GA channels. Thus, we interpret our observation that the order parameter of the bulk lipid in GA/DPPC dispersions levels off at GA/DPPC ratio of 1:15 (cf. Fig. 5) as an indication of dissociation of GA channels in GA/DPPC dispersions. (Note that in the case of positive mismatch and ignoring any dehydration effect, the GA channel would be subject to a compression, which would tend to stabilize the GA channel, contrary to the observed formation of the H_{II} phase).

H_{II} phase formation in GA/DPPC

It was found that in GA/DOPC dispersions with GA/DPPC ratios $>$1:15 GA channels dissociate, GA monomers aggregate due to both the high [GA] and the strong self-association tendency of GA, and an H_{II} phase is induced, in which the preferred GA/DOPC ratio is 1:7, although it can be greater if less lipid is available (Killian et al., 1987). In our experiments we see the effects of GA aggregation for a GA/DPPC ratio $>$1:15 (i.e., for 1:12.5 and 1:5).

First, consider whether we did observe indications of the H_{II} phase formation in our ESR measurements. ^{31}P-NMR studies have shown that GA/DPPC dispersions of a ratio up to 1:10 are in the lamellar phase (Van Echteld et al., 1982), but when the ratio is $>$1:10, an H_{II} phase is observed (Watnick et al., 1990). Given these previous observations, we expect that our results for the 1:5 case are for the H_{II} phase, whereas those for the 1:12.5 case are for a precursor wherein the GA is aggregating, but has not yet formed the H_{II} phase.

Up to now we have emphasized the similarities in our ESR results for the 1:5 and 1:12.5 cases, consistent with the existence of a nonnegligible boundary lipid component characterized by a bent end chain and slower reorientational dynamics. However, a more careful examination of our results does show some significant differences in behavior. For example, we find that order parameters of the boundary lipid in GA/DPPC dispersions of ratio 1:12.5 and 1:5 vary with temperature differently. In the heating cycle for the ratio 1:12.5 there is a step at 40°C in a plot of the order parameters versus the temperature (jumping up from -0.37 at 40°C to -0.17 at 41°C), but no such jump was observed for the ratio of 1:5 (cf. Fig. 8, *top*). This contrast between the two curves of order parameter versus temperature is consistent with the substantial difference in the outer peak

separation versus temperature curves for the GA/DPPC ratios of 1:12.5 and 1:5, which are shown in Fig. 8, *bottom*). The temperature of 40°C, at which a jump in the order parameter occurs, is very close to the gel-to-liquid crystalline phase transition temperature of pure DPPC of 41°C. This seems to indicate that the boundary lipid for a GA/DPPC ratio of 1:12.5 is still in a lamellar phase. In light of our results, we suggest that when the temperature is raised to 40°C, the thermal motion of the acyl chains leads to an effective reduction in their length, reducing the need for the bending of the end chain to accommodate the GA. However, the nearly constant and large negative order parameters (-0.44) over this temperature range observed for the boundary lipid for GA/DPPC ratio 1:5 is more consistent with a stable, e.g., an H_{II} phase, for the boundary lipid, that does not exhibit a "chain melting" transition characteristic for vesicles in the lamellar phase.

Let us now consider the relative amounts of boundary and bulk lipid that we found. Dispersions of an initial GA/DOPC ratio of 1:10 fractionated by sucrose gradient centrifugation generated a ratio of the lamellar phase fraction (GA/DOPC of ratio 1:15) to the H_{II} phase fraction (GA/DOPC of ratio 1:7), 43:56 (Killian et al., 1987, Table 2). From this ratio, a molar ratio of bulk lipid (lamellar phase) to boundary lipid (H_{II} phase) is calculated to be 47:53. This ratio is slightly lower than the ratio of bulk lipid to boundary lipid we obtained from ESR measurement and spectral simulations, i.e., 56:44 for GA/DPPC ratio 1:5 (Table 1). Considering the fact that DOPC has a stronger preference for H_{II} phase formation than DPPC has (Van Echteld et al., 1982), it is reasonable that a larger proportion of lipid partitions into the H_{II} phase in GA/DOPC dispersions than in GA/DPPC dispersions.

Driving force for GA-induced H_{II} phase formation

Now we would like to consider the driving force for H_{II} phase formation induced by GA in terms of the current understanding about the lipid lamellar phase to H_{II} phase transition. It was found that acyl chains are more splayed in the H_{II} phase than in the liquid crystalline phase (Lafleur et al., 1990, 1996; Thurmond et al., 1993) and on average the acyl chain region in the H_{II} phase is more disordered than in the liquid crystalline phase (Lafleur et al., 1996). It was suggested that acyl chain splaying caused by chain disorder may trigger the H_{II} phase formation (Mantsch et al., 1981). Killian et al. (1986) also suggested that the ability to induce a disordering of the lipid acyl chain packing at high [GA] is important for H_{II} phase formation.

Our results, as discussed above, indicate that there is dynamic bending near the end of the acyl chain of the boundary lipid, which is a manifestation of the shrinkage of acyl chains arising from the hydrophobic mismatch between GA and the lipid. We noted in the Introduction that the broad component of the ESR spectra from GA/DPPC dispersions associated with boundary lipid is more prominent in the spectra from 16PC than from 10PC, and not seen in the spectra from 5PC. This indicates that the dynamic bending is most severe at the center of the bilayer and fades away toward the headgroup. That is, acyl chains associated with boundary lipid are more splayed at high [GA] than in pure DPPC membranes. This structural change results in a negative curvature constraint at both leaflets of the bilayer, thus frustrating the bilayers in GA/DPPC dispersions. This is the driving force for the GA-induced H_{II} phase formation (Seddon, 1990; Gruner, 1985). Already, at a GA/DPPC molar ratio of $\sim$1:12.5, a dynamic bending of the end chain segment occurs. This is very likely a precursor state (see above), where the negative curvature constraint in each bilayer is not large enough to induce the H_{II} phase, so the bilayer remains integral until somewhat higher [GA] is present.

Thus, in our view this driving force arises primarily from the combined effect of lipid headgroup dehydration and hydrophobic mismatch between lipid and peptide. The lipid dehydration effect is important, as we discussed above, since dehydration of lipid can cause a hydrophobic mismatch to occur even though it does not appear to be the case before the lipid and the peptide are mixed. It is interesting that a fusion peptide of feline leukemia virus modulates the lipid polymorphism in a similar way to that of GA (Davis et al., 1998). This peptide is very fusogenic and reduces the lamellar-to-H_{II} phase transition temperature of PE to a low peptide/lipid ratio. Most importantly, it does dehydrate the lipid bilayers and disorder the bilayers in a peptide concentration-dependent manner. Therefore, our suggested mechanism for the modulation of DPPC polymorphism by GA might add insight into fusogenic and lipid phase modulation properties of fusion peptides.

Hysteresis: a slow thermally induced structural relaxation process

Let us first highlight some observations we have made with respect to hysteresis. 1) Hysteresis in the cooling versus the heating cycles was only observed for GA/DPPC dispersions of ratio $>$1:15, in which bulk and boundary lipid molecules partition into two different phases, and GA molecules in different phases have different conformations (the CF dimers versus the nonchannel forming aggregates). 2) The outer peak separations of the broad component in the cooling cycles are a little smaller than those in the corresponding heating cycles, which means that the boundary lipid molecules have net smaller negative order parameters in the cooling cycles ($S = -0.39$) than in the corresponding heating cycles ($S = -0.44$). 3) The populations of boundary lipid molecules are smaller in the cooling cycles than in the corresponding heating cycles, which means that there is less boundary lipid associated with the aggregates. Since aggregates appear to prefer a definite ratio of lipids, [e.g., 7 lipids per GA for GA/DOPC (Killian et al., 1987)], this very likely implies less GA aggregation.

Secondly, we have to consider the effect of temperature on the structure of GA/DPPC dispersions. Since upon heating more lipid acyl chain segments will change from all-*trans* conformation to *gauche* conformations, the lengths of the acyl chains will become shorter and the hydrophobic mismatch between GA and DPPC will be lessened. Thus, it is reasonable to assume that this lessening in the hydrophobic mismatch would shift the equilibrium in the direction of more GA and lipid molecules partitioning into the bulk lipid phase. However, we observed these changes only after the dispersions were heated to 75°C, resulting in less aggregate present in the cooling cycles than had been present in the heating cycle. That is, these structural changes lag behind the temperature changes. Thus, the hysteresis is just a manifestation of a thermally induced slow structural relaxation process in the lipid/GA system. The time scale for the temperature change is tens of minutes, whereas the time scale for the structural change is probably hours or even days in the temperature range (between 30° and 45°C) at which the hysteresis was observed.

We expect that the rate-determining step upon heating is the "melting" of the GA aggregates, whereas in the cooling cycle, it is the channel dissociation followed by aggregation of the GA. Our discussion of the previous paragraph is consistent with the "melting" hysteresis occurring, i.e., heating for a period at an elevated temperature is needed to melt aggregates. The latter "supercooling" hysteresis is best demonstrated by observations on the quenched sample (ratio DPPC/GA of 5). It yielded the same boundary lipid fraction for both heating and cooling cycles, and it was about equal to that for the regular cooling cycle. Thus the rapid quenching interfered with the aggregation, so even when this sample was heated, reduced aggregation was observed. Further quenching studies with different ratios of DPPC/GA might provide additional insight.

One matter that still needs some consideration is the nature of GA conformers present at the outset of the heating cycle. We discussed in the Materials and Methods section why in our work [and that of Killian and de Kruijff (1985b), Killian et al. (1987), and Watnick et al. (1990) who use similar procedures] the GA in the lamellar phase is very likely in the CF dimer state, but we cannot yet rule out the presence of some DS dimer. Thus, in our procedure the short period of heating at 75°C could be converting the remaining DS dimer to CF dimer. However, studies by Tournois et al. (1987) strongly suggest that it is the CF conformation of GA that is responsible for its H_{II} phase-inducing activity, which involves CF dimer dissociation and aggregation. If the DS dimer must be converted first to CF dimer for these processes to occur, then we would expect an increase in aggregation for the ensuing cooling cycle, which is the opposite of what we see. Thus the interpretation of our ESR results in the light of the previous studies (Killian and de Kruijff, 1988) is inconsistent with such a hypothesis for the effect of heating.

General considerations of the boundary lipid

We now consider an issue related to a classic problem in magnetic resonance studies of lipid/protein interaction. It has been suggested for decades that the broad components observed in ESR spectra from chain-labeled lipids in protein/lipid complexes represent lipid molecules in contact with the protein molecules, i.e., the boundary lipids (Jost et al., 1973; Knowles et al., 1979; Marsh and Watts, 1982; Marsh, 1989; Griffith et al., 1986; Devaux and Seigneuret, 1985). These broad components have large outer peak separations, usually >60 G. Their rotational diffusion rates were estimated to be approaching the rigid limit on the ESR time scale (Marsh, 1989). Therefore, boundary lipid molecules were considered to be immobilized. When the protein/lipid ratio is high, the outer peak separation of the broad component is temperature-independent, and this has led to a suggestion that spin-labeled lipid is being trapped between aggregated proteins (Devaux and Seigneuret, 1985; Chapman et al., 1977). However, such an immobilized component was not detected by ^{2}H-NMR measurements (Seelig et al., 1982). This discrepancy is usually interpreted as a result of the difference in time scale between the ESR and NMR techniques (Marsh, 1985) and estimating exchange rates between the boundary and bulk lipids (Marsh, 1985; 1989). Despite these efforts, the question of how the lipid phase structure is affected and modulated by membrane proteins is not yet clear.

In this study we observed large and temperature-independent outer peak separations from GA/DPPC dispersions at molar ratio 1:5. Our simulations are consistent with this spectral feature resulting from the dynamic bending of end chain segments of boundary lipid molecules. Comparisons between our data and the published phase structure of GA/lipid dispersions revealed that these boundary lipid molecules could be organized into an H_{II} phase. It is quite possible that the broad component in the ESR spectra from some other protein/lipid complexes may also have a large negative order parameter, resulting from dynamic bending of end chain segments of the boundary lipids (or other structural change induced by interactions with the proteins). The mobility of these lipids is substantially reduced, but they are not immobilized. It is not unreasonable to conclude that such boundary lipids also would have a different phase structure from the bulk lipids.

In previous ESR studies the number of lipid molecules immobilized by each protein molecule was calculated for a given protein/lipid system, and it was associated with the stoichiometry and specificity of protein/lipid interactions (for reviews see Marsh, 1985; Devaux and Seigneuret, 1985). These matters may need to be reexamined in those cases wherein the following considerations may be relevant. 1) The broad component does not necessarily represent completely immobilized lipid molecules. 2) Proteins may aggregate at high concentrations, the size and the form of protein aggregates (linear chains, cross-linked chains, or lumps) may be different for different protein/lipid systems.

3) Protein aggregates and monomers may partition into different lipid phases, in which protein/lipid ratios may be different. 4) The relative amounts of the different phases may vary with the overall protein/lipid ratio. Therefore, for such cases those numbers may not reflect the actual number of lipid molecules in contact with each protein molecule. However, the molar ratios of protein to lipid in the bulk and boundary lipid phases, which might not readily be obtained just from analyzing ESR spectra, but could be determined by other means, can help to determine the phase structure of the lipids. A good example is the compositional analysis of GA/DOPC dispersions by the sucrose density centrifugation experiment (Killian et al., 1987), which we used (in the above) to support our hypothesis that the boundary lipid in GA/DPPC dispersions of ratio 1:5 is very likely in the H_{II} phase.

CONCLUSIONS

Our ESR spectral observations and least-squares simulations are consistent with the aggregation of GA molecules in DPPC dispersions when the GA/DPPC molar ratio is >1: 15. The aggregation of GA ultimately results in boundary lipids appearing in a new phase, an H_{II} phase, which coexists with the bulk lipid phase. The lipids in the boundary lipid phase are characterized by substantially reduced motion and a large negative order parameter at the end chain. The effect of GA on the bulk lipid is smaller, but not negligible. The large negative order parameter for the chain-labeled lipid, 16PC, indicates a significant bending of the end chain segment, which could result from hydrophobic mismatch between the GA channel and the DPPC molecule. Additional studies by 2D-FT-ESR, with its greater ability to discern ordering and dynamics, are recommended to confirm and strengthen these conclusions, once the sensitivity to boundary lipid of this technique is sufficiently enhanced.

Of most relevance to the lipid/peptide interactions is the property of GA to destabilize the bilayer structure. That is, a combination of the dehydration effect of GA and the hydrophobic mismatch between GA and lipid bilayers might be a driving force for H_{II} phase formation.

We thank Professor David E. Budil for his help and advice during the early stages of this work, Dr. Zhichun Liang for performing the 2D-FT-ESR simulations for us, Dr. Richard H. Crepeau for helpful discussions, and Dr. Jeff Barnes for his help in plotting the orientational probability distribution functions.

This work was supported by National Institutes of Health Grant GM25862.

REFERENCES

Boni, L. T., T. P. Stewart, and S. W. Hui. 1984. Alterations in phospholipid polymorphism by polyethylene glycol. *J. Membr. Biol.* 80:91–104.

Borbat, P. P., R. H. Crepeau, and J. H. Freed. 1997. Multifrequency two-dimensional Fourier transform ESR: an X/Ku-band spectrometer. *J. Magn. Reson.* 127:155–167.

Bouchard, M., J. H. Davis, and M. Auger. 1995. High speed magic angle spinning solid-state ^{1}H nuclear magnetic resonance study of the conformation of gramicidin A in lipid bilayers. *Biophys. J.* 69:1933–1938.

Budil, D. E., S. Lee, S. Saxena, and J. H. Freed. 1996. Nonlinear-least-squares analysis of slow-motion EPR spectra in one and two dimensions using a modified Levenberg-Marquardt algorithm. *J. Magn. Reson. A.* 120:155–189.

Chapman, D., B. A. Cornell, A. W. Eliasz, and A. Perry. 1977. Interactions of helical polypeptide segments which span the hydrocarbon region of lipid bilayers. Study of the gramicidin A lipid-water system. *J. Mol. Biol.* 113:517–538.

Chapman, D., J. C. Gomez-Fernandez, and F. M. Goni. 1979. Intrinsic protein-lipid interactions. Physical and biochemical evidence. *FEBS Lett.* 98:211–223.

Cornell, B. A., L. E. Wier, and F. Separovic. 1988. The effect of gramicidin A on phospholipid bilayers. *Eur. Biophys. J.* 16:113–119.

Cortijo, M., A. Alonso, J. C. Gomez-Fernandez, and D. Chapman. 1982. Intrinsic protein-lipid interactions: infrared spectroscopic studies of gramicidin A, bacteriorhodopsin and Ca^{2+}-ATPase in biomembranes and reconstituted systems. *J. Mol. Biol.* 157:597–618.

Crepeau, R. H., S. Saxena, S. Lee, B. Patyal, and J. H. Freed. 1994. Studies on lipid membranes by two-dimensional Fourier transform ESR: enhancement of resolution to ordering and dynamics. *Biophys. J.* 66: 1489–1504.

Davis, S. M., R. F. Epand, J. P. Bradshaw, and R. M. Epand. 1998. Modulation of lipid polymorphism by the feline leukemia virus fusion peptide: implications for the fusion mechanism. *Biochemistry*. 37: 5720–5729.

de Kruijff, B., P. R. Cullis, A. J. Verkleij, M. J. Hope, C. J. A. Van Echteld, T. F. Taraschi, P. Van Hoogevest, J. A. Killian, A. Rietveld, and A. T. M. Van Der Steen. 1985. Modulation of lipid polymorphism by lipid-protein interactions. *In* Progress in Protein-Lipid Interactions, Vol. 1. A. Watts and J. J. H. H. M. De Pont, editors. Elsevier Scientific Publishers, New York.

Devaux, P. F., and M. Seigneuret. 1985. Specificity of lipid-protein interactions as determined by spectroscopic techniques. *Biochim. Biophys. Acta.* 822:63–125.

Earle, K. A., J. K. Moscicki, M. Ge, D. E. Budil, and J. H. Freed. 1994. 250 GHz-ESR studies of polarity gradients along the aliphatic chains in phospholipid membranes. *Biophys. J.* 66:1213–1221.

Fattal, D. R., and A. Ben-Shaul. 1993. A molecular model for lipid-protein interaction in membrane: the role of hydrophobic mismatch. *Biophys. J.* 65:1795–1809.

Freed, J. H. 1994. Field gradient ESR and molecular diffusion in model membranes, *Annu. Rev. Biophys. Biomol. Struct.* 23:1–25.

Ge, M., D. E. Budil, and J. H. Freed. 1994. ESR studies of spin-labeled membranes aligned by isopotential spin-dry ultracentrifugation: lipid-protein interactions. *Biophys. J.* 67:2326–2344.

Ge, M., and J. H. Freed. 1993. An electron spin resonance study of interactions between gramicidin A' and phosphatidylcholine bilayers. *Biophys. J.* 65:2106–2123.

Ge, M., and J. H. Freed. 1998. Polarity profiles in oriented and dispersed phosphatidylcholine bilayers are different. An ESR study. *Biophys. J.* 74:910–917.

Griffith, O. H., D. A. McMillen, J. F. W. Keana, and P. C. Jost. 1986. Lipid-protein interactions in cytochrome c oxidase. A comparison of covalently attached phospholipid photo-spin-label with label free to diffuse in the bilayer. *Biochemistry*. 25:574–584.

Gruner, S. M. 1985. Intrinsic curvature hypothesis for biomembrane lipid composition: a role for nonbilayer lipid. *Proc. Natl. Acad. Sci. USA.* 82:3665–3669.

Helfrich, P., and E. Jakobsson. 1990. Calculation of deformation energies and conformations in lipid membranes containing gramicidin channels. *Biophys. J.* 57:1075–1084.

Henis, Y. I. 1993. Role of viral glycoprotein mobility in Sendai virus-mediated cell fusion. *In* Viral Fusion Mechanism. J. Bentz, editor. CRC Press, Boca Raton, FL. 335–361.

Holowka, D., and B. Baird. 1996. Antigen-mediated IgE receptor aggregation and signaling: a window on cell surface structure and dynamics. *Annu. Rev. Biophys. Biomol. Struct.* 25:79–112.

Jost, P. C., O. H. Griffith, R. A. Capaldi, and G. A. Vanderkooi. 1973. Evidence for boundary lipid in membranes. *Proc. Natl. Acad. Sci. USA.* 70:480–484.

Kahn, C. R., K. L. Baird, D. B. Jarrett, and J. S. Flier. 1978. Direct demonstration that receptor crosslinking or aggregation is important in insulin action. *Proc. Natl. Acad. Sci. USA.* 75:4209–4213.

Kar, L., E. Ney-Igner, and J. H. Freed. 1985. Electron spin resonance and electron-spin-echo study of oriented multilayers of L_α-dipalmitoylphosphatidylcholine water system. *Biophys. J.* 48:569–595.

Ketchem, R. R., W. Hu, and T. A. Cross. 1993. High-resolution conformation of gramicidin A in a lipid bilayer by solid-state NMR. *Science*. 261:1457–1460.

Killian, J. A. 1992. Gramicidin and gramicidin-lipid interactions. *Biochim. Biophys. Acta*. 1113:391–425.

Killian, J. A., K. N. J. Burger, and B. de Kruijff. 1987. Phase separation and hexagonal H_{II} phase formation by gramicidins A, B and C in dioleoylphosphatidylcholine model membranes. A study on the role of the tryptophan residues. *Biochim. Biophys. Acta*. 897:269–284.

Killian, J. A., and B. de Kruijff. 1985a. Thermodynamic, motional, and structural aspects of gramicidin-induced hexagonal H_{II} phase formation in phosphatidylethanolamine. *Biochemistry*. 24:7881–7890.

Killian, J. A., and B. de Kruijff. 1985b. Importance of hydration for gramicidin-induced hexagonal H_{II} phase formation in dioleoylphosphatidylcholine model membranes. *Biochemistry*. 24:7890–7898.

Killian, J. A., and B. de Kruijff. 1988. Proposed mechanism for H_{II} phase induction by gramicidin in model membranes and its relation to channel formation. *Biophys. J.* 53:111–117.

Killian, J. A., C. W. van den Berg, H. Tournois, S. Keur, A. J. Slotboom, G. J. M. van Scharrenburg, and B. de Kruijff. 1986. Gramicidin-induced hexagonal H_{II} phase formation in negative charged phospholipids and the effect of N- and C-terminal modification of gramicidin on its interaction with zwitterionic phospholipids. *Biochim. Biophys. Acta*. 857:13–27.

Knowles, P. F., A. Watts, and D. Marsh. 1979. Spin-labeled studies of lipid immobilization in dimyristoylphosphatidylcholine-substituted cytochrome oxidase. *Biochemistry.* 18:4480–4487.

Ladbrooke, B. D., R. M. Williams, and D. Chapman. 1968. Studies on lecithin-cholesterol-water interactions by differential scanning calorimetry and x-ray diffraction. *Biochim. Biophys. Acta.* 150:333–340.

Lafleur, L., M. Bloom, E. F. Eikenberry, S. M. Gruner, Y. Han, and P. R. Cullis. 1996. Correlation between lipid plane curvature and lipid chain order. *Biophys. J.* 70:2747–2757.

Lafleur, M., P. R. Cullis, B. Fine, and M. Bloom. 1990. Comparison of the orientational order of lipid chains in the L_α and H_{II} phases. *Biochemistry*. 29:8325–8333.

Lee, D. C., A. A. Durrani, and D. Chapman. 1984. A difference infrared spectroscopic study of gramicidin a, alamethicin and bacteriorhodopsin in perdeuterated dimyristoylphosphatidylcholine. *Biochim. Biophys. Acta*. 769:49–56.

Lee, S., B. R. Patyal, S. Saxena, R. H. Crepeau, and J. H. Freed. 1994. Two-dimensional Fourier-transform electron spin resonance in complex fluids. *Chem. Phys. Lett.* 221:397–406.

Mantsch, H. H., A. Martin, and D. Cameron. 1981. Characterization by infrared spectroscopy of the bilayer to nonbilayer phase transition of phosphatidylethanolamines. *Biochemistry.* 20:3138–3145.

Marsh, D. 1985. ESR spin label studies of lipid-protein interactions. *In* Progress in Protein-Lipid Interactions, Vol. 1. A. Watts and J. J. H. H. M. de Pont, editors. Elsevier, Amsterdam. 143–172.

Marsh, D. 1989. Experimental methods in spin-label spectral analysis. *In* Biological Magnetic Resonance. Spin Labeling: Theory and Application, Vol. 9. L. J. Berliner and J. Reuben, editors. Plenum Press, New York. 255–303.

Marsh, D., and A. Watts. 1982. Spin labeling and lipid-protein interactions in membranes. *In* Lipid-Protein Interactions. P. C. Jost and O. H. Griffith, editors. John Wiley & Sons, New York. 53–126.

McIntosh, T. J., and S. A. Simon. 1994. Hydration and steric pressure between phospholipid bilayers. *Annu. Rev. Biophys. Biomol. Struct*. 23:27–51.

Meirovitch, E., A. Nayeem, and J. H. Freed. 1984. Analysis of protein-lipid interactions based on model simulations of electron spin resonance spectra. *J. Phys. Chem.* 88:3454–3465.

Mou, J., D. M. Czajkowsky, and Z. Shao. 1996. Gramicidin A aggregation in supported gel state phosphatidylcholine bilayers. *Biochemistry*. 35: 3222–3226.

Parsegian, V. A., N. Fuller, and R. P. Rand. 1979. Measured work of deformation and repulsion of lecithin bilayers. *Proc. Natl. Acad. Sci. USA.* 76:2750–2754.

Patyal, B. R., R. H. Crepeau, and J. H. Freed. 1997. Lipid-protein interactions using two-dimensional Fourier-transform electron spin resonance. *Biophys. J.* 73:2201–2220.

Rand, R. P., and V. A. Parsegian. 1989. Hydration forces between phospholipid bilayers. *Biochim. Biophys. Acta.* 988:351–376.

Rice, D., and E. Oldfield. 1979. Deuterium nuclear magnetic resonance studies of the interaction between dimyristoylphosphatidylcholine and gramicidin A'. *Biochemistry.* 18:3272–4279.

Robertson, D., D. Holowka, and B. Baird. 1986. Cross-linking of immunoglobulin E-receptor complexes induces their interaction with the cytoskeleton of rat basophilic leukemia cells. *J. Immunol.* 136:4565–4572.

Schneider, D. J., and J. H. Freed. 1989. Calculating slow motional magnetic resonance spectra. *In* Biological Magnetic Resonance, Vol. 8. L. J. Berliner and J. Reuben, editors. Plenum Press, New York. 1–76.

Schreiber, A. B., T. A. Libermann, I. Lax, Y. Yarden, and J. Schlessinger. 1983. Biological role of epidermal growth factor clustering. *J. Biol. Chem.* 258:846–853.

Seddon, J. M. 1990. Structure of the inverted hexagonal (H_{II}) phase, and non-lamellar phase transitions of lipids. *Biochim. Biophys. Acta.* 1031: 1–69.

Seelig, J., N. Seelig, and L. Tamm. 1982. Nuclear magnetic resonance and lipid-protein interactions. *In* Lipid-Protein Interactions, Vol. 2. P. C. Jost and O. H. Griffith, editors. John Wiley & Sons, New York. 127–148.

Shin, Y.-K., and J. H. Freed. 1989. Thermodynamics of phosphatidylcholine-cholesterol mixed model membranes in the liquid crystalline state studied by the orientational order parameter. *Biophys. J.* 56:1093–1100.

Short, K. W., B. A. Wallace, R. A. Myers, S. P. A. Fodor, and A. K. Dunker. 1987. Comparison of lipid/gramicidin dispersions and cocrystals by Raman scattering. *Biochemistry.* 26:557–562.

Simon, S. A., T. J. McIntosh, and R. Latorre. 1982. Influence of cholesterol on water penetration into bilayers. *Science.* 216:65–67.

Tanaka, H., and J. H. Freed. 1985. Electron spin resonance studies of lipid-gramicidin interactions utilizing oriented multibilayers. *J. Phys. Chem.* 89:350–360.

Thurmond, R. L., G. Lindblom, and M. F. Brown. 1993. Curvature, order, and dynamics of lipid hexagonal phases studied by deuterium NMR spectroscopy. *Biochemistry.* 32:5394–5410.

Tournois, H., C. H. J. P. Fabrie, K. N. J. Burger, J. Mandersloot, P. Hilgers, H. van Dalen, J. de Gier, and B. de Kruijff. 1990. Gramicidin A induced fusion of large unilamellar dioleoylphosphatidylcholine vesicles and its relation to the induction of type II nonbilayer structure. *Biochemistry.* 29:8297–8307.

Tournois, H., J. A. Killian, D. W. Urry, O. R. Bokking, J. de Gier, and B. de Kruijff. 1987. Solvent determined conformation of gramicidin affects the ability of the peptide to induce hexagonal H_{II} phase formation in DOPC model membranes. *Biochim. Biophys. Acta.* 905:222–226.

Van Echteld, C. J. A., B. de Kruijff, A. J. Verkleij, J. Leunissen-Bijvelt, and J. de Gier. 1982. Gramicidin induces the formation of non-bilayer structures in phosphatidylcholine dispersions in a fatty acid chain length dependent way. *Biochim. Biophys. Acta.* 692:126–138.

Van Echteld, C. J. A., R. van Stigt, B. de Kruijff, J. Leunissen-Bijvelt, A. J. Verkleij, and J. de Gier. 1981. Gramicidin promotes formation of the hexagonal H_{II} phase in aqueous dispersions of phosphatidylethanolamine and phosphatidylcholine. *Biochim. Biophys. Acta.* 648:287–291.

Wallace, B. A., and R. W. Janes. 1991. Co-crystals of gramicidin A and phospholipid. A system for studying the structure of a transmembrane channel. *J. Mol. Biol.* 217:625–627.

Watnick, P. I., S. I. Chan, and P. Dea. 1990. Hydrophobic mismatch in gramicidin A'/lecithin systems. *Biochemistry.* 29:6215–6221.

Xing, J., and H. L. Scott. 1992. Monte Carlo studies of a model for lipid-gramicidin A bilayers. *Biochim. Biophys. Acta.* 1106:227–232.

Yeagle, P. L. 1985. Cholesterol and the cell membrane. *Biochim. Biophys. Acta.* 822:267–287.